JACS
JOURNAL OF THE AMERICAN CHEMICAL SOCIETY

ARTICLE

pubs.acs.org/JACS

Doping Cu in Semiconductor Nanocrystals: Some Old and Some New Physical Insights

Bhupendra B. Srivastava, Santanu Jana, and Narayan Pradhan*

Department of Materials Science and Centre for Advanced Materials, Indian Association for the Cultivation of Science, Jadavpur 700032, India

Supporting Information

ABSTRACT: Cu-doped inorganic semiconductors with concomitant optical properties have garnered enormous research interest in the last two decades. However, uncertainties over the origin of Cu emission, its oxidation state, resemblance with trap state emission, position of Cu d-state, emission spectral width, and moreover understanding of the doping mechanism restricted the wide development of the synthetic methodology for high-quality Cu-doped nanocrystals. It has been shown recently that the emission from Cu-doped semiconductor nanocrystals can span over a wide spectral window and could be a potential color tunable dispersed nanocrystal emitter. Herein, we report the size and composition of variable Cu-doped ZnS/$Zn_{1-x}Cd_xS$ zinc-blende (ZB) surface alloyed nanocrystals with intense, stable, and tunable emission covering the blue to red end of the visible spectrum. Further, the Cu dopant emission is distinguished from trap state emission, and the composition variable spectral broadening has been justified on the account of a different environment around the Cu ions in the host lattice. Whereas some findings are in agreement with past reports, several new physical insights presented here would help the community for an in-depth mechanistic study on Cu doping. Moreover, these doped nanocrystal emitters can be a promising candidate for application ranging from optoelectronics to bio-labeling.

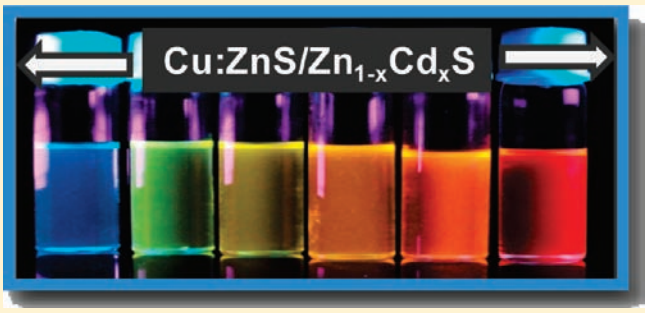

INTRODUCTION

Transition metal ions-doped semiconductor nanocrystals are emerging as a lucrative alternative to semiconductor quantum dots with tunable, intense, and stable emission in visible as well as in near-IR spectral window for different optoelectronic applications.[1] Minimized self-absorption,[1c,1d,2] higher excited-state lifetime,[3] emission spectral width,[1d,1g,3a] and thermal stability[1g,2] are the unique properties of this new series of nanocrystals making these doped nanocrystals as important as quantum dots. Insertion of transition metal dopants (e.g., Mn, Cu ions, etc.) creates intermediate energy state/s between the valence and conduction band of host semiconductor nanocrystal and changes its photophysical relaxation process.[1a−1c,1f−1k,2−4] As a result, the dopant emission evolves with new optical properties whose nature and position vary with that of chosen hosts and dopants. For Mn-doped nanocrystals, the dopant emission has been restricted within the yellow-orange spectral window,[1a,1c,1d,2,5] but in case of Cu doping, a wide range of tunable emission has been observed due to the tunability of the size of the hosts.[1d,1g] As compared to the Mn-doped system, the study of Cu doping is still in a very nascent stage, even though it was reported decades before.[6] The origin of this Cu dopant emission, reasons for its higher intensity, tunability of emission, possibility of involving Cu d-states, emission spectral width, and several other associated properties have led to many questions, which are not yet resolved. There are several reports in the literature with contradicting remarks, which puzzle the whole story and create hurdles for the possible development of such useful tunable visible light emitting nanocrystals.

The first problem to be encountered is with the oxidation state of Cu ions in the doped semiconductor system, as argument over the existence of Cu (I)[7] and Cu(II)[3a,3c,8] has been continuing for a long time period with support for both states. Cu(II) salts are being used as the dopant source,[1d,3a,3c,7a,7b,8a,8c] which generates a strong belief that the Cu(II) ions retain their +2 oxidation state after being doped in group II−VI semiconductors. Moreover, in some cases for ZnS and CdS hosts, it has been reported that sulfide ions reduce Cu(II) to Cu(I), which is confirmed by EPR measurement, thus establishing Cu(I) as a stable oxidation state for these systems.[7a,7b,9] Hence, these contradicting statements over the Cu oxidation state create problems in establishing the mechanism of the Cu dopant emission, and detailed scientific studies are needed to understand the photophysical process of these doped nanocrystals.

Second, the exact position of the Cu d energy levels between the valence and conduction band of the host semiconductor nanocrystals is also not clear until now. Tunable Cu doping with tuning the size of host suggests that the Cu d levels must lie

Received: October 5, 2010
Published: December 27, 2010

dx.doi.org/10.1021/ja1089809 | J. Am. Chem. Soc. 2011, 133, 1007–1015

between the valence and conduction band of the host nanocrystals, which takes part in the recombination process. From different literature reports, the most acceptable photophysical mechanism has been predicted involving Cu T_2 states, which stay above the valence band, and after excitation the valence hole transfers to this T_2 state.[6a,7b,8a,8c,10] The recombination then follows with the electron in the conduction band and hole in Cu state, and consequently tunable emission with the change in the band gap of the host is observed. On the contrary, another report suggests the Cu state remains just below the conduction band of the host nanocrystals and takes part in the recombination process by transferring the electrons from this Cu state to the valence band of the host.[7a] Moreover, whether these proposed mechanisms are generic or vary with the nature of semiconductors is not yet clear. Literature reports on Cu-doped nanocrystal hosts show, for example, ZnS results in blue-green emission,[3e,11] in ZnSe it is a little more extended to greenish yellow spectral window,[1d,3a] in CdS it is orange-red,[8a,10j] and recently in InP,[1g] it has been extended to near IR. On the basis of these reports, we have summarized that the tentative position of the Cu states falls close to the valence band for various semiconductor nanocrystals shown in Figure 1, which indicates the Cu state position varies from one semiconductor to other. However, variations in the position of the Cu d-state with change in the composition of host, dopant environmental position in lattice, etc., are not yet established. A more ideal system with proper tuning of band gap, composition, and size is required to study in detail the exact position of Cu states and origin of the tunable dopant emission.

Third, the nature of the Cu dopant emission is also confusing. For different host semiconductors, for example, ZnS, CdS, ZnSe, InP, etc., the position, tunability, and broad nature of Cu dopant emission resemble the surface state emission of respective host nanocrystals.[1d,1g,8a,11] All of these similarities create doubt over the origin of the emission that it is from the surface trap or if it really involves Cu d-state as reported in the literature. In case of Cu-doped ZnSe with tunable emission, the intensity (above 40% QY), thermal stability, and also the higher lifetime provide some impression that this emission is different from surface trap state emission.[1d,3a] Yet its large emission width (70−90 nm) is still confused with trap state emission.[1d,1g]

Fourth, the selective adsorption of the Cu dopant at different facets of the host nanocrystal is not clear. Analogous to Mn,[4a] whether Cu dopant also needs suitable facets of the host crystal lattice for adsorption or it can be adsorbed irrespective of the crystal structure of hosts is still not investigated. From the literature, it indicates that zinc blende ZnS[11] and ZnSe[1d] and wurtzite CdS[10d] and CdSe[10a] nanocrystals can be doped with Cu. Therefore, it is difficult to predict the crystal phase-dependent doping possibility for Cu dopants.

Hence, the doping of Cu and the involved photophysical process for the dopant emission are still puzzling with so many uncertainties, and more experimental as well as theoretical support is needed to understand the hidden basic fundamental science behind this. Nonetheless, stable and intense emission associated with several new properties would enable these materials for different practical applications like bioimaging, LED fabrication, etc. By using group II−VI semiconductors, which are well studied and have well-developed syntheses, we report the possible Cu doping in II−VI alloyed nanocrystals (Cd−Zn−S) to achieve control over the emission evolution and tunability in entire visible window. The possible crystal phase requirement for the dopant adsorption, distinguishing surface and internal doped Cu systems, excited-state lifetime decay, and time delay photoluminescence spectra are also studied and reported in this Article where some findings agree with existing literature report and some provide new information.

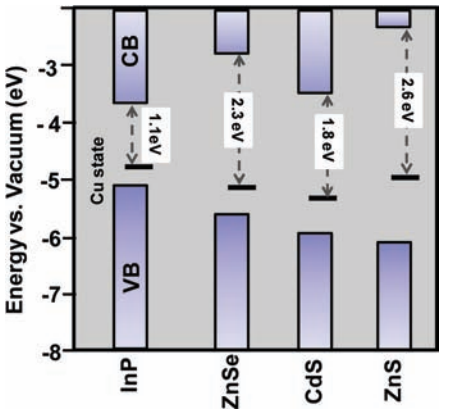

Figure 1. Bulk band gap and position of the Cu state close to the valence band in InP, ZnSe, CdS, and ZnS nanocrystals. The Cu state positions are collected from various literature references.[1d,1g,7b,8a] In case of Cu-doped semiconductors having tunable emission (e.g., ZnSe), the lowest emission energy position has been taken as the Cu energy state.

RESULTS AND DISCUSSION

Designing Host Semiconductor Nanocrystals for Cu Doping. According to Figure 1, the position of the Cu d-energy level is not fixed but rather varies with the nature of semiconductor hosts.[1d,1g,7b,8a] However, as it falls between the valence and conduction band of a particular host nanocrystal, Cu state related emission is always expected at a lower energy position as compared to the band edge absorption. Following this principle, a wide variety of semiconductor nanocrystals can be expected to generate tunable dopant emission in different spectral window once they get successfully doped with Cu. To study details of the evolution mechanism of the Cu dopant emission, we confine our synthesis for a particular II−VI semiconductor host, which would provide widely tunable dopant emission with distinguishable dopant related optical properties. The ideal case would be of CdS nanocrystals, which has the band edge exactly required to provide size tunable dopant emission that spans over entire visible range. Yet several reports on Cu-doped CdS nanocrystals show that its tunability is restricted to a short-range yellow-orange window.[8a,10j] We also failed to achieve the tunability of emission covering the entire visible window by doping Cu in CdS nanocrystals synthesized using the literature method[12] following high temperature colloidal technique. The other suitable host might be the alloy of Cd, Zn, and S, which also possess the ideal band edge absorption to achieve the wide tunable dopant emission with required composition as a possible alternative.[13] In addition, the alloy nanocrystals would also provide the information of both size and composition tunable doping effect, which would help to identify the exact Cu state position and the possible origin of the photophysical process. While following different literature reports on Cd, Zn, and S alloyed nanocrystals[4e,13a] and introducing molecular Cu precursor during growth/alloying, we failed to achieve significant dopant emission as expected. Close analysis of the alloy formation indicates that these nanocrystals have wurtzite (WZ) crystal structure. As per the recent development of Mn dopant adsorption

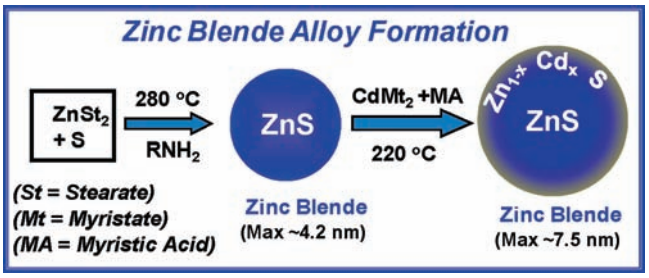

Figure 2. Schematic representation of formation of surface alloyed nanocrystals of Zn, Cd, and S with ZnS core and $Zn_{1-x}Cd_xS$ shell. Initially, ZnS nanocrystals are synthesized using the literature reported method, and then the calculated amount of cadmium precursor is injected for the alloyed shell growth.

mechanism, where Mn prefers zinc blende (ZB) surfaces for preferable adsorption,[4a] we also tried to modify the synthetic procedure to design ZB alloyed nanocrystals. On successful designing of size and composition tunable ZB Cd, Zn, and S alloyed nanocrystals, Cu is successfully doped during growth and annealing, providing stable, intense, and tunable emission extending over entire visible window. Moreover, as it provides emission tuning and composition variable broadening, it would be helpful to understand the fundamental science behind the Cu doping. Hence, considering this newly developed alloyed nanocrystals as a model host, we have studied different involved physical insights to establish the origin of Cu dopant emission. However, at this stage, we could not conclude the exact reason of Cu doping in only ZB semiconductor nanocrystals, and it needs further investigation.

Synthesis of ZB Alloyed Zn−Cd−S Host Nanocrystals. Among the most popular synthetic methodologies, for nucleation and growth of spherical nanocrystals, CdS mostly forms WZ[12,14] and ZnS forms ZB[15] crystal phase. In normal alloy formation conditions, fast reactivity of Cd with S leads to the nucleation of WZ CdS nanocrystals. Moreover, the higher chemical reactivity of Cd than Zn enriches Cd population in the alloyed nanocrystals that leads to growth in WZ phase.[16] Hence, to design the ZB alloyed structures needs more architectural control and balanced reactivity of the precursors.

To avoid both nucleation of WZ seeds and the possible cation exchange during growth and/or alloying, we have designed here a new methodology to synthesize ZB alloyed nanocrystals. The method follows cubic ZnS seed mediated surface alloy formation after addition of the appropriate amount (to avoid separate nucleation of CdS) of Cd precursor during growth. Initial Zn precursor concentration taken in the reaction mixture is also important as it restricts the possible cation exchange by Cd. Figure 2 shows a schematic presentation for the synthesis of ZB surface alloy of Zn, Cd, and S (ZnS core and $Zn_{1-x}Cd_xS$ surface). In a typical synthesis, nearly 4.2 nm diameter of ZnS seed nanocrystals was synthesized following our previous reported method,[3e] and the appropriate amount of cadmium myristate solution has been injected at 220 °C. Continuous annealing at this temperature tunes the band edge of the nanocrystals with simultaneous alloying and growth. Figure 3a−c shows the TEM images of seed ZnS and surface alloyed nanocrystal during continuous growth/alloying. XRD (Figure 3d) supports ZB structure throughout the annealing. Shifting of ZB ZnS peaks toward ZB CdS supports the formation of alloyed structure. Surface alloying has been supported by etching and successive ICP measurements (Supporting Information Table S1). Figure 3e shows the blue shift of the absorption band edge, indicating reduction in the size of the alloyed nanocrystals during etching process. Decrease in elemental ratio of Cd to Zn during etching was observed, which eventually ends up with no Cd atom concentration, suggesting the nanocrystal has surface alloyed structure. Also, after the completion of the reaction (i.e., no tuning in emission position), the final ∼6.5 nm nanocrystals show a Zn:Cd ratio of 4:1 having an absorption band edge ∼450 nm, but according to literature reported[13] homogeneous alloyed nanocrystal having ∼450 nm band edge shows a Zn:Cd ratio of 1:3, which indicates our synthesized nanocrystals are not homogeneous but surfacely alloyed having ZnS in the core. Moreover, blue shifting of XRD peaks (figure not shown) of etched sample confirms the center is mostly populated with ZnS.

The growth of the alloyed structure on ZnS seeds follows here a chemical activation process by cadmium precursor. In our reaction condition, seed ZB ZnS can grow maximum up to ∼4.2 nm (average) despite the presence of excess Zn and S precursors at 300 °C injection and 260 °C growth temperature. Increase of temperature for the possible activation of zinc precursor (zinc stearate) rather agglomerates these nanocrystals but does not help them to grow beyond this size. Yet injection of cadmium to this reaction mixture (at the reduced temperature of 220 °C to avoid the self-nucleation of CdS) triggers the growth and alloying. Myristate salt of cadmium has been chosen for effective growth at this reduced temperature. We investigated that at this temperature zinc stearate precursor is activated in the presence of Cd-myristate with excess of myristic acid. In fact, myristic acid activates zinc as well as S precursor,[17] and they are precipitated along with Cd during the growth leading to surface alloyed ZB nanocrystals. This excess of activated zinc precursor helps to suppress the displacement of Zn from seed ZnS by more reactive Cd.

Further, the composition variable band gap tuning of this surface alloyed nanocrystals in which the center is confined with pure ZnS and the surface is the alloyed one differed from the homogeneous alloying.[13,18] It is important to point out that there is no weak quantum confinement effect (QCE) observed like Zhong et al. reported on Cd−Zn−S alloyed nanocrystals,[13a] which is indicated by the absorption spectra (Figure 4a, left panel) despite the small bulk Bohr radius of CdS and ZnS (typical exciton Bohr radii of ZnS and CdS are 2.2 and 3.0 nm).[19] A similar observation has been reported by Ouyang et al. for the small sized Cd−Zn−S alloyed nanocrystals.[20] Also, the band gap derived from the absorption edge does not match with the band gap of homogeneous alloy calculated according to the alloy band gap equation[13b,21] based on the effective mass model for a particular composition. This indicates ∼1.5−2 nm growth of alloy on seed ZnS surface controls the entire band gap tunability of the system. This is further supported by the rapid red shift of the ZnS band edge (∼50 nm) soon after the Cd injection. Therefore, the change of band gap mostly depends on the composition of surface alloy and not on the whole nanocrystal. The position of the Cu band and tunability of the Cu emission in association of the host tunable band gap have been predicted as per the results obtained and discussed in the later part of this Article.

Doping Process and Spectral Evolution. We have adopted here the growth doping strategy[1d,3e] to dope the ZB alloyed nanocrystals, where dopant ions are allowed to adsorb on the host seed nanocrystals and then nanocrystals are further grown

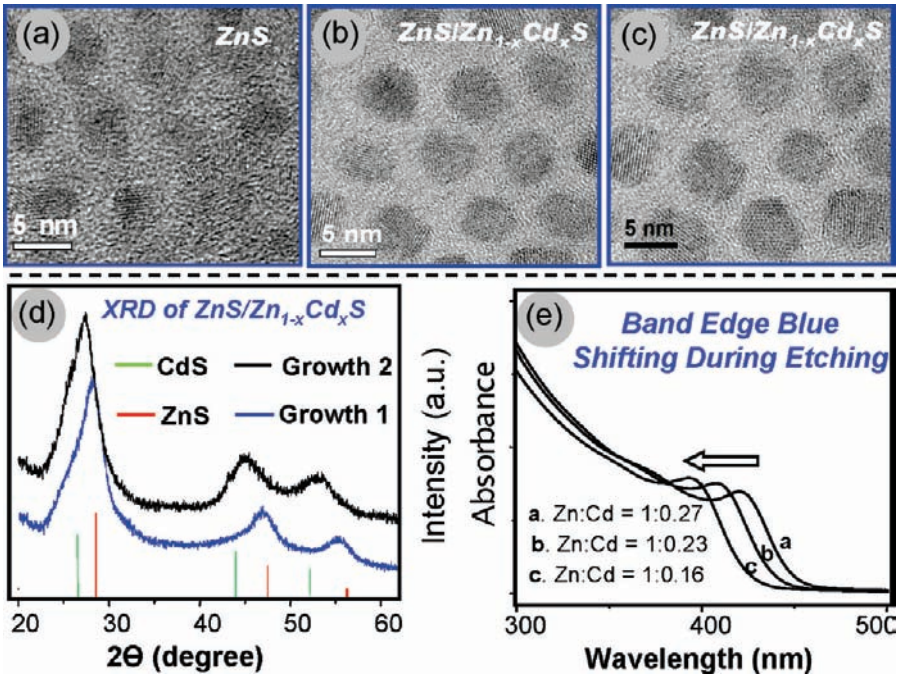

Figure 3. (a−c) Transmission electron microscopic (TEM) images of seed ZnS and successive stages during alloy growth. (d) XRD of two surface alloyed nanocrystals during successive alloying and growth. Shifting of the peak positions from ZnS side toward CdS indicates alloying of nanocrystals. (e) Successive UV−visible spectra of the surface alloyed nanocrystals during the etching process. Significant blue shift of the band edge suggests for reducing the size of nanocrystals.

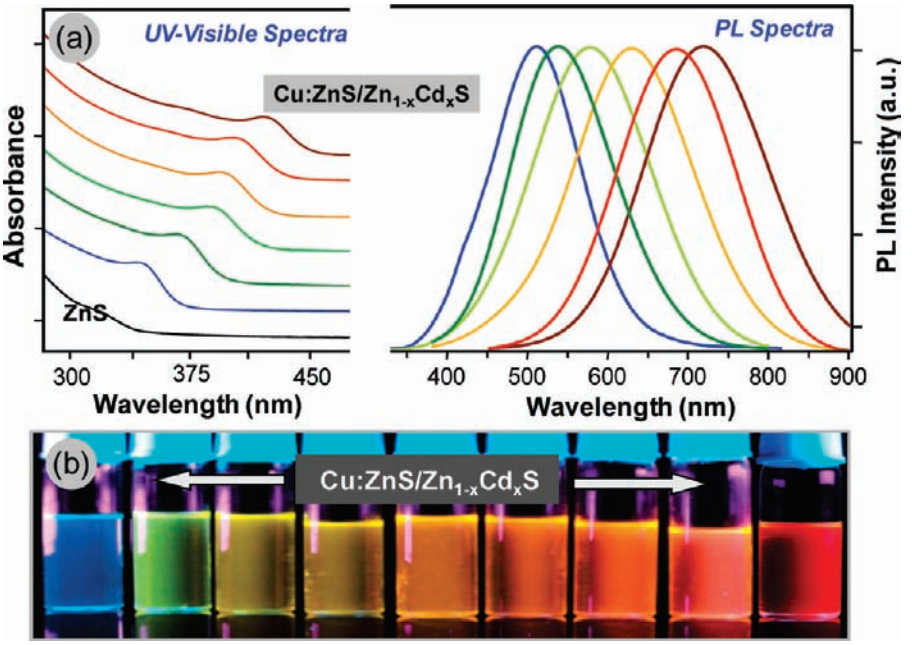

Figure 4. (a) Evolution of UV−visible (left panel) and corresponding photoluminescence (right panel) during doping of Cu in the alloyed nanocrystals. The bottom spectrum (black line) of the left panel indicates for ZnS seeds only before injection of dopant Cu source. Excitation wavelength is 365 nm. (b) Digital picture of samples collected in a typical experiment from different stages of the doping process of the alloyed nanocrystals. These are excited using a hand-held UV lamp at 350 nm excitation.

along with alloying to bury the adsorbed dopant ions and keep them away from the surface of nanocrystals. After formation of ZnS seeds (∼4.2 nm), the reaction temperature has been reduced to 220 °C, and molecular Cu precursor (Cu-sterate in octadcene) has been introduced (∼1.5% of zinc) dropwise to the reaction system. The required amount of Cd stock solution (see Supporting Information, SI) has then been injected at the same temperature, and the progress of the reaction is monitored spectrophotometrically. Within a few seconds, the dopant emission appears, and with the progress of alloying

dx.doi.org/10.1021/ja1089809 |J. Am. Chem. Soc. 2011, 133, 1007–1015

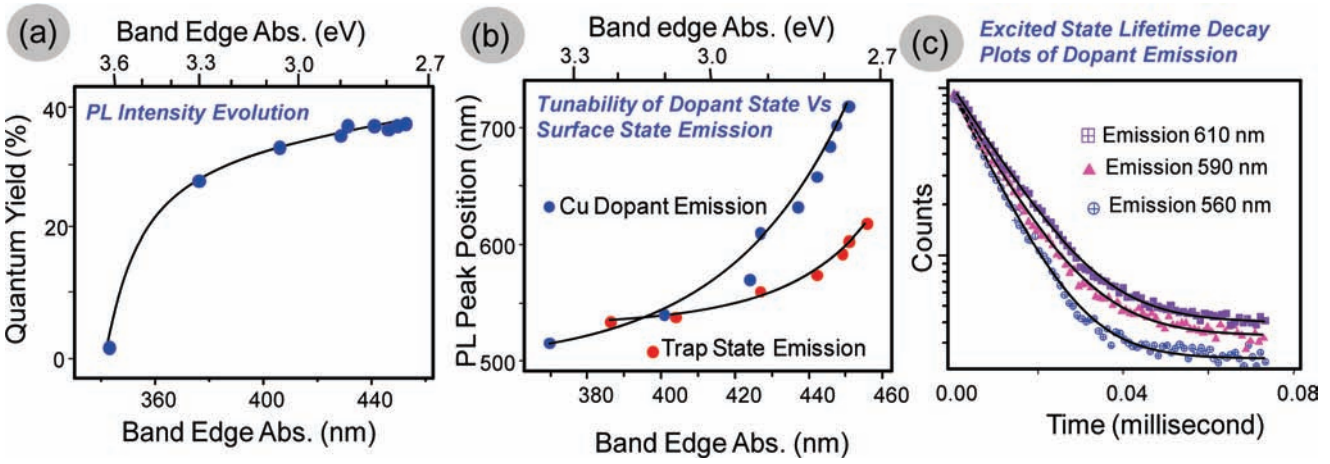

Figure 5. (a) Quantum yield (QY) of doped alloyed nanocrystals versus the band edge absorbance (Abs.) shifting during successive alloying and growth. (b) Change of the emission peak position of Cu dopant emission and surface trap emission with tuning of the band edge of alloyed nanocrystals. (c) Excited-state lifetime decay plots of the dopant emission at different emission center.

and growth, it intensifies, broadens, and red shifts from ~500 to 680 nm (Figure 4a, right panel). The UV−visible spectra (Figure 4a, left panel) indicate that the band edge of the nanocrystals moves along with the tuning of the emission. A digital picture of Cu-doped alloyed nanocrystals under UV excitation is shown in Figure 4b. The best quantum yield (QY) of the dopant emission has been observed as 38%, but average reactions show 20−30% QY.

To know whether this intense and tunable emission originated from Cu center or from trap state, a chemical sensing experiment has been carried out for surface doped alloyed nanocrystals. A mixture of trioctylphosphine (TOP) and oleylamine (OA) has been used to clean out Cu from the nanocrystals surface. From a typical synthesis, soon after the evolution of dopant emission, the reaction mixture was taken out and treated in a chemical bath of the mixture of TOP and OA. Within minutes during stirring the emission completely quenched without reducing the nanocrystals size, and this suggests that the emission is coming because of the involvement of Cu dopant center. Yet for internally doped nanocrystals, the sample taken out after successive alloyed layer growth did not quench the emission with the surface cleaning process. After Cu was cleaned out from the surface doped nanocrystals, when Cu is reinjected following the doping process, the intense dopant emission again evolutes and red shifts with the progress of the reaction. This confirms that Cu states are responsible for this emission. A similar kind of surface cleaning for Co^{2+}-doped ZnO nanocrystals has also been done by Schwartz et al. with trioctylphosphineoxide (TOPO) to clean out the Co^{2+} ions.[22] In accordance with all these facts, our system agrees with several other reports[1d,7b,8a] in the literature that the host exciton recombines via the Cu impurity state providing broad, intense, tunable emission at longer wavelength than the band edge absorption.

Adsorption of Cu Dopant and the Doping Process. Figure 5a shows a typical evolution process of the dopant emission, which follows a sharp enhancement of the emission soon after the cadmium addition. Even in the presence of excess Zn and S precursors in the reaction mixture, the growth and alloying just starts after the Cd injection, which evolutes and enhances the dopant emission. This suggests that Cu ions, which were introduced to ZnS seeds, precipitated along with Cd, Zn, and S precursors. Further overgrowth of host nanocrystals does not significantly enhance the emission intensity. Therefore, the emission evolution process for the Cu dopant mostly depends on the adsorption of dopant ions and is different from traditional quantum dots where the excitonic emission slowly enhances with growth, reaches a maximum, and then reduces. This is noted here that a very small amount of Cu ions (~0.8% of the total cations) are introduced for effective Cu doping as their dilution in the reaction mixture prevents them from forming CuS nanocrystals, but with increase of concentration, black colored CuS[7b] nanocrystals nucleate and grow, which interfere in the doping process. We have found that the sample that gives the highest quantum yield contains ~0.6−0.8% (with respect to total cation concentration) Cu dopant concentration confirmed from ICP. All these measurements in Figure 5a were carried out in situ without further purification. The purification process quenches the surface dopant emission and not the internal one, which is a general phenomenon in doped dots. Hence, we can conclude that the dopant emission intensity significantly changes for the surface and internally doped nanocrystals.

Surface Trap State versus Cu State Emission. Even though intense and wide range tunable emission from doped alloyed nanocrystals signifies the involvement of Cu centers, its position and broadening are very often confused with the surface state related emission.[3a] To distinguish between these two factors, we have performed a controlled reaction of the alloyed system without Cu addition for comparison (Figure S1). Under identical reaction time, there is a wide difference in the tunability range (Figure 5b) for the less intense trap state emission and highly intense Cu dopant emission. Also, at high temperature (280 °C), the disappearance of trap state emission of the undoped surface alloyed nanocrystals due to annealing effect[13a] and less effect on emission intensity of Cu-doped alloyed nanocrystals show significant distinct origins for these two channels. Further, the excited-state lifetime (discussed in a later section) completely distinguishes Cu dopant emission from the trap state. Table S2 gives the comparison of similarities and differences of both dopant and trap state emission.

Excited-State Lifetime Decay of Dopant Emission. The excited-state lifetime of the dopant emission at various positions has been measured to identify its origin. Normally, lifetime of the excitonic emission as well as the surface emission for various semiconductor nanocrystals falls in order of one and few tens nanoseconds (ns), respectively,[23] whereas for doped nanocrystals in which an additional energy state has been incorporated by

dx.doi.org/10.1021/ja1089809 |J. Am. Chem. Soc. 2011, 133, 1007–1015

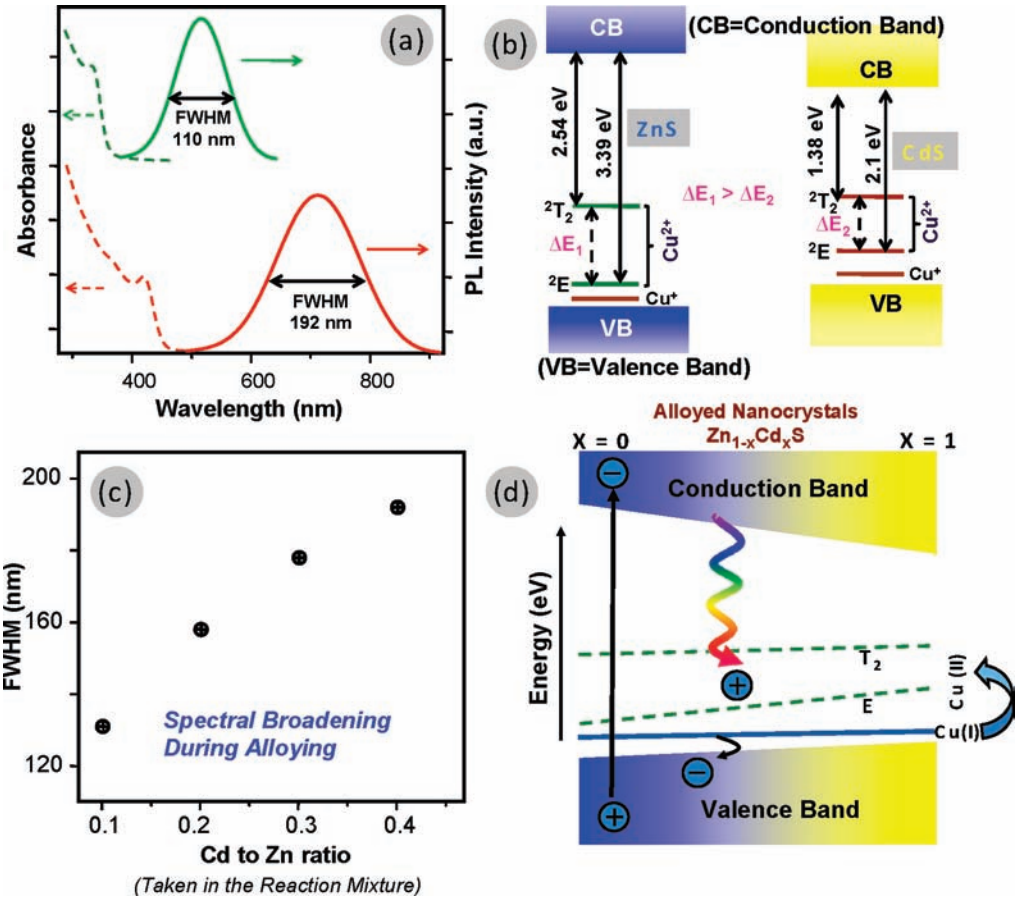

Figure 6. (a) Two representative UV−vis and PL spectra of Cu-doped alloyed nanocrystals showing significant difference in their PL full-width at half maxima (fwhm). (b) Schematic representation of the possible energy states of Cu in ZnS and CdS semiconductor hosts. (c) Composition tunable spectral broadening. Change of fwhm of the dopant emission during growth and annealing of the alloyed nanocrystals. The ratio of Cd to Zn has been calculated from ICP measurements. (d) Schematic representation of different Cu states during conversion of Cu(I) to Cu(II) in the composition variable alloyed nanocrystals and the possible recombination process.

dopant is expected to have a longer excited-state lifetime. For Cu-doped ZnSe, the lifetime has been reported in order of hundred nanoseconds, and it changes with tuning the emission position.[3a] We have also observed the microsecond order excited-state lifetime of the Cu dopant emission for these alloyed host nanocrystals, and it increases with alloying and growth (Figure 5c). Further time delay PL measurement has been carried out to compare the origin of Cu dopant and surface trap emission. One and five microsecond (μs) time delay PL measurements for emission centered at ~645 nm retain the dopant emission, which indicates it originates from dopant related channel but not from the related trap whose lifetime falls within ~90 ns. Hence, the wide difference of excited-state lifetime of dopant emission from the trap state completely distinguishes its origin with the involvement of Cu state.

Oxidation State of Cu and Possible Mechanism of Exciton Recombination. To understand the exciton recombination process, the oxidation state of Cu in the nanocrystal is very important. As Cu(I) d^{10} and Cu(II) d^9 have different electronic configurations, electron paramagnetic resonance (EPR) spectra of the alloyed doped nanocrystals were measured to identify the presence of unpaired electron of Cu. No EPR signal has been observed, which suggests the absence of Cu(II) (Figure S3). Yet the EPR of molecular precursor used for doping (Cu(II)stearate) in the control measurement shows a signal indicating its paramagnetic behavior. Hence, even Cu−II precursors are used for doping, and the absence of any EPR signal in the doped nanocrystals supports the presence of Cu-I, which is expected from the reduction of Cu(II) in the reaction system. This result also overlaps with earlier reports of Isarov et al., which have suggested the reduction of Cu-II to Cu-I by anion (sulfides) present in the nanocrystals.[7a]

In the presence of Cu-I, the recombination of the exciton generated from host nanocrystal involves two possible radiative processes. One involves transfer of Cu d-state electron to the valence hole, and the other process occurs with the conduction electron transfer to this hole trapped Cu-d state. Between these two processes, the dopant emission depends upon the one that is more favorable. For semiconductor nanocrystals, when the band gap changes the movement observed in the conduction band is much more than the valence band because of the small effective mass of the electron compare to the hole.[24] As band gap change is seen as a shift in conduction band,[24] the recombination process that occurs through the second process, which involves conduction electron transfer to the hole trapped Cu-d state, can only give the wide tunable dopant emission. It rules out the radiative recombination possibility of the Cu-d state to valence hole. Further, the energy corresponding to the dopant emission gives the energetic location of the Cu-d states in the band gap that is found closer to the valence band for our host

dx.doi.org/10.1021/ja1089809 |J. Am. Chem. Soc. 2011, 133, 1007–1015

nanocrystals, which also agrees with some previous reports explaining the energetic location of Cu-d states in II−VI semiconductor nanocrystals.[7b,8a,10e,25]

Change in the Nature of Emission Spectra during Annealing/Growth. One of the important features of the Cu dopant emission is the broad emission spectra as compared to the normal excitonic emission of quantum dots. Generally, in undoped quantum dots, emission broadening is observed due to particle size distribution, and hence in case of these Cu-doped alloy nanocrystals the particle size distribution-dependent broadening is also expected. To investigate this, photoluminescence excitation (PLE) spectra have been measured at different positions for a particular dopant emission spectrum (Figure S4), and no significant change has been observed, suggesting the sample has a narrow particle size distribution, which is also supported by TEM (Figure 3b,c). This clearly suggests that the broadness of this spectrum is not due to the size distribution of host nanocrystals. In these doped alloyed nanocrystals, the generated exciton transfers its valence hole to the filled higher potential Cu (I) d-state and changes it to Cu (II), which has two different energy states $T_2(D)$ and $E(D)$. Both these two energy states have the possibility to accept the excited electron from the conduction band of the host nanocrystals, which may broaden the corresponding emission spectra.[6a,10e,25]

One of the prominent examples for Cu-doped semiconductor nanocrystals is Cu-doped ZnSe, which is the first of its kind that provides tunable intense dopant emission. When the dopant emission nature has been analyzed throughout the reaction process, a significant difference in the dopant PL fwhm was not observed.[1d] Yet in our particular alloy case, we have observed a continuous change in dopant emission broadening during the reaction process (Figure 4a and 6a). We have analyzed the dopant Cu d-energy level differences and their effect on the dopant emission spectra for ZnS and CdS nanocrystals. The energy difference is found as ∼0.86 eV (∼123 nm) and ∼0.71 eV (∼308 nm) for ZnS and CdS, respectively (Figure 6b).[10e,25] This indicates that the emission spectral broadening (with respect to wavelength scale) is governed by these two Cu d states energy difference and is expected higher for CdS than for ZnS. As our host nanocrystals are alloys of Zn, Cd, and S, it should show continuous broadening with increase of Cd content. Figure 6c shows the composition variable change in PL fwhm from ∼100 to ∼200 nm, and this trend agrees with the above prediction. From this observation, we can assume that the lattice environment around the dopant Cu when changed from pure Zn neighbors to both Zn and Cd (Figure S5), the energy difference between the two Cu states changes, and that results in the continuous broadening of dopant emission. A schematic presentation of the exciton relaxation mechanism has been shown in Figure 6d. In a recent report on Cu-doped InP with ZnSe interface, Xie et al. have also shown the Cu dopant PL fwhm closely match with the energy difference of the Cu states.[1g] As observed for the Cu-doped system, the energy difference of the two Cu-d states and movement of the host conduction band is mostly responsible for the radiative emission. This dopant emission depends on the nature, composition, and size of semiconductor nanocrystals, which could also be the associative reason for this broadening of the PL spectra. Furthermore, lattice vibration in these alloyed nanocrystals may also be responsible to some extent in this emission broadening for this unique nature of Cu dopant. However, more experimental results, extension to other systems, and importantly theoretical supports are necessary for better understanding of different electronic processes and change of spectral nature.

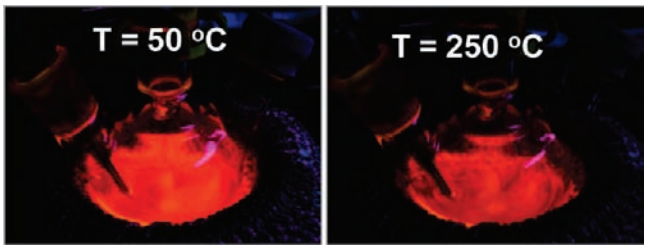

Figure 7. Temperature effects of Cu-doped alloyed nanocrystal shown by visual observation, confirming the doped nanocrystals are thermally stable.

Thermal Stability and Processability of Cu-Doped Nanocrystals. As reported above, the emission for the Cu dopant is associated with the Cu energy level (Figure 6d), and therefore it should be less coupled with lattice vibration in comparison to the excitonic of undoped semiconductor nanocrystals. Visually, these Cu-doped alloyed nanocrystals did not show a significant change in emission upon heating to 250 °C, whereas (Figure 7) generally undoped quantum dots suffer almost complete quenching of its band gap PL[1g] at about 150 °C. After heating to 300 °C, the emission intensity of the d-dots also showed some noticeable decrease, although this decrease in emission at 300 °C is found to be reversible. When the sample was cooled to room temperature, the emission intensity was almost recovered.

Further, these doped nanocrystal emitters can be transferred to the water without losing the emission intensity significantly following the common surface modification process.[3e] The emission is stable both in aqueous and in nonaqueous dispersions, and no further surface modification treatment (for example, thiol or S) is necessary as in the Cu-doped selenide system.

CONCLUSION

We report here the efficient, stable, and water-soluble Cu-doped nanocrystals with emission tunable in the entire visible window by incorporating Cu dopant in ZB surface alloyed ZnS/$Zn_{1-x}Cd_xS$ nanocrystals. In addition, mechanism of dopant adsorption, its emission evolution, and different associated photophysical insights are studied. The main findings of this Article are as follows. First, the adsorption of Cu dopant is facilitated on the ZB crystal phase of the host ZnS/$Zn_{1-x}Cd_xS$ surface alloyed nanocrystals. Second, the emission positions, extent of emission tunability, remarkable enhancement of intensity, longer excited-state lifetime, and existence of time delay PL of the dopant emission clearly distinguish it from surface state emission. Third, the oxidation state of Cu and its position between the valence and conduction band for this particular alloy system are investigated, and a possible electron−hole relaxation mechanism is predicted. Fourth, dopant related emission broadening is associated with the composition distribution of the alloyed nanocrystals. The above findings would give a better paradigm of the understanding of Cu doping in semiconductor nanocrystals, which is the first ever doped system developed so far with emission spanning over the entire visible window. Moreover, the results presented here agree with several old concepts of Cu doping, that is, emission broadening, tunability, presence of Cu(I), etc., and also provide some new information, that is, composition variable spectral broadening,

crystal phase selective dopant adsorption, wide range of spectral tunability over the entire visible window, and definite supports that well distinguish Cu dopant emission from surface state emission, which will help the community to investigate different veiled fundamental aspects of Cu doping in future.

EXPERIMENTAL SECTION

Synthesis of Zinc Blende Alloyed Nanocrystals. Initially, small sized ZnS nanocrystals were synthesized following the procedure reported in reference 3e. In a typical synthesis, 0.063 g of $Zn(St)_2$, 0.012 g of S powder, and 0.6 g of ODA are loaded in a 50 mL three-necked flask along with 10 mL of ODE. The reaction mixture was degassed for 15 min by purging with argon. The reaction flask was then heated to 270 °C and annealed for 5 min and then cooled to 220 °C. After that, 2 mL of cadmium myristate stock (see SI) was swiftly injected to the reaction mixture at same temperature. The reaction mixture was further annealed, and samples were taken out for measurements at different time intervals. Synthesized nanocrystals were precipitated by using excess of acetone from ODE and further purified by choosing chloroform as solvent and acetone as nonsolvent.

Doping Cu in Alloyed Nanocrystals. For Cu doping in alloyed nanocrystals, 0.1 mL of $Cu(St)_2$ stock solution (see SI) was added dropwise at 220 °C temperature before addition of cadmium myristate in the above synthesis and annealed for 30 min. After that, the reaction was followed as stated in above procedure.

Surface Cleaning of Doped Nanaocrystals. For the specific etching of Cu ion doped on the surface of nanocrystal, a TOP−OA (1:1) mixture was used as the etching agent. In a typical experiment, purified nanocrystals having an OD of 0.3 at 350 nm were taken in 2 mL of TOP−OA mixture and heated at 180 °C for the desired time and then cooled to room temperature and then again purified with acetone−methanol mixture. For stepwise surface cleaning, the desired times were chosen as 5, 10, and 20 min. We have observed 20 min is sufficient for complete surface cleaning at our chosen temperature of 180 °C.

Etching of Nanocrystals. Benzoyl peroxide was chosen as an etching agent for these doped nanocrystals. In a typical procedure, the doped nanocrystals after repeated purification were dispersed in chloroform, and a calculated amount of benzoyl peroxide (0.1 mmol with nanocrystals solution having OD 0.3 at 380 nm) was added to this reaction mixture under vigorous stirring. 0.2 mmol of oleic acid also was added to be a counterion of etched metal ions. After 20 min of stirring, the UV−visible spectra of doped nanocrystals, such as doped ZnS/$Zn_{1-x}Cd_xS$ systems, were found to be ∼8 nm blue-shifted. Next, the solution was collected at a certain temperature and precipitated with acetone. Precipitated nanocrystals were again purified and reprecipitated for ICP measurement.

ASSOCIATED CONTENT

Supporting Information. Materials, instrumentation, and supporting figures. This material is available free of charge via the Internet at http://pubs.acs.org.

AUTHOR INFORMATION

Corresponding Author
camnp@iacs.res.in

ACKNOWLEDGMENT

B.B.S. and S.J. contributed equally to this work. DST of India is acknowledged for funding. B.B.S. and S.J. acknowledge CSIR, India, and N.P. acknowledges LNJ Bhilwara for fellowships. We acknowledge Prof. D. D. Sarma for helpful discussions.

REFERENCES

(1) (a) Bhargava, R. N.; Gallagher, D.; Hong, X.; Nurmikko, A. *Phys. Rev. Lett.* **1994,** *72*, 416–419. (b) Sooklal, K.; Cullum, B. S.; Angel, S. M.; Murphy, C. J. *J. Phys. Chem.* **1996,** *100*, 4551–4555. (c) Norris, D. J.; Yao, N.; Charnock, F. T.; Kennedy, T. A. *Nano Lett.* **2001,** *1*, 3–7. (d) Pradhan, N.; Goorskey, D.; Thessing, J.; Peng, X. *J. Am. Chem. Soc.* **2005,** *127*, 17586–17587. (e) Santra, S.; Holloway, P. H.; Stanley, J. T.; Mericle, R. A. *J. Am. Chem. Soc.* **2005,** *127*, 1656–1657. (f) Yang, Y.; Chen, O.; Angerhofer, A.; Cao, Y. C. *J. Am. Chem. Soc.* **2006,** *128*, 12428–12429. (g) Xie, R.; Peng, X. *J. Am. Chem. Soc.* **2009,** *131*, 10645–10651. (h) Vlaskin, V. A.; Janssen, N.; van Rijssel, J.; Beaulac, R.; Gamelin, D. R. *Nano Lett.* **2010,** *10*, 3670–3674. (i) Zeng, R.; Rutherford, M.; Xie, R.; Zou, B.; Peng, X. *Chem. Mater.* **2010,** *22*, 2107–2113. (j) Acharya, S.; Sarma, D. D.; Jana, N. R.; Pradhan, N. *J. Phys. Chem. Lett.* **2010,** *1*, 485–488. (k) Martyshkin, D. V.; Fedorov, V. V.; Kim, C.; Moskalev, I. S.; Mirov, S. B. *J. Opt.* **2010,** *12*, 024005/1–024005/5.

(2) Pradhan, N.; Peng, X. *J. Am. Chem. Soc.* **2007,** *129*, 3339–3347.

(3) (a) Jana, S.; Srivastava, B. B.; Acharya, S.; Santra, P. K.; Jana, N. R.; Sarma, D. D.; Pradhan, N. *Chem. Commun.* **2010,** *46*, 2853–2855. (b) Beaulac, R.; Ochsenbein, S. T.; Gamelin, D. R. *Nanocrystal Quantum Dots*, 2nd ed.; Taylor & Francis: New York; 2010; pp 397−453. (c) Bol, A. A.; Ferwerda, J.; Bergwerff, J. A.; Meijerink, A. *J. Lumin.* **2002,** *99*, 325–334. (d) Gan, C.; Zhang, Y.; Battaglia, D.; Peng, X.; Xiao, M. *Appl. Phys. Lett.* **2008,** *92*, 241111/1–241111/3. (e) Srivastava, B. B.; Jana, S.; Karan, N. S.; Paria, S.; Jana, N. R.; Sarma, D. D.; Pradhan, N. *J. Phys. Chem. Lett.* **2010,** *1*, 1454–1458.

(4) (a) Erwin, S. C.; Zu, L.; Haftel, M. I.; Efros, A. L.; Kennedy, T. A.; Norris, D. J. *Nature* **2005,** *436*, 91–94. (b) Norris, D. J.; Efros, A. L.; Erwin, S. C. *Science* **2008,** *319*, 1776–1779. (c) Archer, P. I.; Santangelo, S. A.; Gamelin, D. R. *J. Am. Chem. Soc.* **2007,** *129*, 9808–9818. (d) Beaulac, R.; Archer, P. I.; van Rijssel, J.; Meijerink, A.; Gamelin, D. R. *Nano Lett.* **2008,** *8*, 2949–2953. (e) Nag, A.; Chakraborty, S.; Sarma, D. D. *J. Am. Chem. Soc.* **2008,** *130*, 10605–10611. (f) Yuhas, B. D.; Zitoun, D. O.; Pauzauskie, P. J.; He, R.; Yang, P. *Angew. Chem., Int. Ed.* **2006,** *45*, 420–423. (g) Yang, Y.; Chen, O.; Angerhofer, A.; Cao, Y. C. *J. Am. Chem. Soc.* **2008,** *130*, 15649–15661. (h) Chen, D.; Ong, G. L.; Xie, R.; Balasubramaninan, M.; Peng, X. *J. Am. Chem. Soc.* **2009,** *131*, 9333–9339. (i) Bhargava, R. N. *J. Lumin.* **1996,** *70*, 85–94. (j) Azad Malik, M.; O'Brien, P.; Revaprasadu, N. *J. Mater. Chem.* **2001,** *11*, 2382–2386. (k) Nag, A.; Sapra, S.; Nagamani, C.; Sharma, A.; Pradhan, N.; Bhat, S. V.; Sarma, D. D. *Chem. Mater.* **2007,** *19*, 3252–3259. (l) Chin, P. T. K.; Stouwdam, J. W.; Janssen, R. A. J. *Nano Lett.* **2009,** *9*, 745–750.

(5) Pradhan, N.; Battaglia, D. M.; Liu, Y.; Peng, X. *Nano Lett.* **2007,** *7*, 312–317.

(6) (a) Peka, P.; Schulz, H. J. *Physica B: Condens. Matter* **1994,** *193*, 57–65. (b) Suyver, J. F.; van der Beek, T.; Wuister, S. F.; Kelly, J. J.; Meijerink, A. *Appl. Phys. Lett.* **2001,** *79*, 4222–4224. (c) Hoffmann, A.; Broser, I.; Thurian, P.; Heitz, R. *J. Cryst. Growth* **1990,** *101*, 532–535. (d) Holton, W. C.; De Wit, M.; Watts, R. K.; Estle, T. L.; Schneider, J. *J. Phys. Chem. Solids* **1969,** *30*, 963–977.

(7) (a) Isarov, A. V.; Chrysochoos, J. *Langmuir* **1997,** *13*, 3142–3149. (b) Corrado, C.; Jiang, Y.; Oba, F.; Kozina, M.; Bridges, F.; Zhang, J. Z. *J. Phys. Chem. A* **2009,** *113*, 3830–3839. (c) Konishi, K.; Hiratani, T. *Angew. Chem., Int. Ed.* **2006,** *45*, 5191–5194. (d) Tang, A.; Yi, L.; Han, W.; Teng, F.; Wang, Y.; Hou, Y.; Gao, M. *Appl. Phys. Lett.* **2010,** *97*, 033112/1–033112/3. (e) Li, J.; Zhang, J. Z. *Coord. Chem. Rev.* **2009,** *253*, 3015–3041.

(8) (a) Mandal, P.; Talwar, S. S.; Major, S. S.; Srinivasa, R. S. *J. Chem. Phys.* **2008,** *128*, 114703/1–114703/7. (b) Yang, P.; Lu, M.; Xu, D.; Yuan, D.; Zhou, G. *Appl. Phys. A: Mater. Sci. Process.* **2001,** *73*, 455–458. (c) Kim, J.-U.; Kim, Y. K.; Yang, H. *J. Colloid Interface Sci.* **2009,** *341*, 59–63.

(9) Sambasivam, S.; Sathyaseelan, B.; Raja Reddy, D.; Reddy, B. K.; Jayasankar, C. K. *Spectrochim. Acta, Part A* **2009,** *71A*, 1503–1506.

(10) (a) Singh, S. B.; Limaye, M. V.; Lalla, N. P.; Kulkarni, S. K. *J. Lumin.* **2008,** *128*, 1909–1912. (b) Sang, W.; Qian, Y.; Min, J.; Li, D.; Wang, L.; Shi, W.; Liu, Y. *Solid State Commun.* **2002,** *121*, 475–478. (c) Zheng, J.; Zheng, Z.; Gong, W.; Hu, X.; Gao, W.; Ren, X.; Zhao, H.

Chem. Phys. Lett. **2008,** *465*, 275–278. (d) Nishidate, K.; Sato, T.; Matsukura, Y.; Baba, M.; Hasegawa, M.; Sasaki, T. *Phys. Rev. B: Condens. Matter* **2006,** *74*, 035210/1–035210/8. (e) Peka, P.; Schulz, H. J. *Solid State Commun.* **1994,** *89*, 225–228. (f) Huang, J.; Yang, Y.; Xue, S.; Yang, B.; Liu, S.; Shen, J. *Appl. Phys. Lett.* **1997,** *70*, 2335–2337. (g) Meulenberg, R. W.; Van Buuren, T.; Hanif, K. M.; Willey, T. M.; Strouse, G. F.; Terminello, L. J. *Nano Lett.* **2004,** *4*, 2277–2285. (h) Que, W.; Zhou, Y.; Lam, Y. L.; Chan, Y. C.; Kam, C. H.; Liu, B.; Gan, L. M.; Chew, C. H.; Xu, G. Q.; Chua, S. J.; Xu, S. J.; Mendis, F. V. C. *Appl. Phys. Lett.* **1998,** *73*, 2727–2729. (i) Khosravi, A. A.; Kundu, M.; Jatwa, L.; Deshpande, S. K.; Bhagwat, U. A.; Sastry, M.; Kulkarni, S. K. *Appl. Phys. Lett.* **1995,** *67*, 2702–2704. (j) Stouwdam, J. W.; Janssen, R. A. J. *Adv. Mater.* **2009,** *21*, 2916–2920. (k) Viswanatha, R.; Chakraborty, S.; Basu, S.; Sarma, D. D. *J. Phys. Chem. B* **2006,** *110*, 22310–22312.

(11) Peng, W. Q.; Cong, G. W.; Qu, S. C.; Wang, Z. G. *Opt. Mater.* **2006,** *29*, 313–317.

(12) Yu, W. W.; Peng, X. *Angew. Chem., Int. Ed.* **2002,** *41*, 2368–2371.

(13) (a) Zhong, X.; Feng, Y.; Knoll, W.; Han, M. *J. Am. Chem. Soc.* **2003,** *125*, 13559–13563. (b) Li, Y.; Ye, M.; Yang, C.; Li, X.; Li, Y. *Adv. Funct. Mater.* **2005,** *15*, 433–441.

(14) Steckel, J. S.; Zimmer, J. P.; Coe-Sullivan, S.; Stott, N. E.; Bulovic, V.; Bawendi, M. G. *Angew. Chem., Int. Ed.* **2004,** *43*, 2154–2158.

(15) Joo, J.; Na, H. B.; Yu, T.; Yu, J. H.; Kim, Y. W.; Wu, F.; Zhang, J. Z.; Hyeon, T. *J. Am. Chem. Soc.* **2003,** *125*, 11100–11105.

(16) (a) Zhong, X.; Feng, Y.; Zhang, Y.; Gu, Z.; Zou, L. *Nanotechnology* **2007,** *18*, 385606/1–385606/6. (b) Regulacio, M. D.; Han, M.-Y. *Acc. Chem. Res.* **2010,** *43*, 621–630.

(17) Karan, N. S.; Mandal, A.; Panda, S. K.; Pradhan, N. *J. Phys. Chem. C* **2010,** *114*, 8873–8876.

(18) Zhong, X.; Liu, S.; Zhang, Z.; Li, L.; Wei, Z.; Knoll, W. *J. Mater. Chem.* **2004,** *14*, 2790–2794.

(19) (a) Krishna, M. V. R.; Friesner, R. A. *J. Chem. Phys.* **1991,** *95*, 8309–8322. (b) Yoffe, A. D. *Adv. Phys.* **1993,** *42*, 173–266.

(20) Ouyang, J.; Ratcliffe, C. I.; Kingston, D.; Wilkinson, B.; Kuijper, J.; Wu, X.; Ripmeester, J. A.; Yu, K. *J. Phys. Chem. C* **2008,** *11*, 4908–4919.

(21) Bawendi, M. C.; Steigerwald, M. L.; Brus, L. E. *Annu. Rev. Phys. Chem.* **1990,** *41*, 477–496.

(22) Schwartz, D. A.; Norberg, N. S.; Nguyen, Q. P.; Parker, J. M.; Gamelin, D. R. *J. Am. Chem. Soc.* **2003,** *125*, 13205–13218.

(23) (a) Califano, M.; Franceschetti, A.; Zunger, A. *Nano Lett.* **2005,** *5*, 2360–2364. (b) Zhang, J.; Zhang, X.; Zhang, J. Y. *J. Phys. Chem. C* **2009,** *113*, 9512–9515.

(24) (a) Robel, I.; Kuno, M.; Kamat, P. V. *J. Am. Chem. Soc.* **2007,** *129*, 4136–4137. (b) Sapra, S.; Sarma, D. D. *Phys. Rev. B: Condens. Matter* **2004,** *69*, 125304/1–125304/7.

(25) Heitz, R.; Hoffmann, A.; Thurian, P.; Broser, I. *J. Phys.: Condens. Matter* **1992,** *4*, 157–168.